

Effects of subtle and dramatic changes to initial conditions on a jet's turbulent structure, mixing and combustion

G. J. Nathan¹, J. Mi¹, G. J. R. Newbold¹, D. S. Nobes¹ and Z.T. Alwahabi²

Schools of Mechanical¹ and Chemical² Engineering, The University of Adelaide, South Australia 5005, Australia

Abstract

Turbulent jet diffusion flames have been widely studied and have also found wide application in industrial burners. However, subtle or dramatic differences often exist between the configurations investigated by different research groups, and also between those investigated in laboratories and those used in industrial burner designs. Although the importance of initial conditions is well established as a general principal, many details of these influences are still only emerging. The present paper reviews previous work, and presents new results, of the effect of such differences on the non-reacting scalar field and on flames. Subtle differences are those arising from a round pipe, a smoothly contracting nozzle and sharp-edged orifice plate. Dramatic differences are generated by large-scale, unsteady precession of the emerging jet. The differences are related to the underlying large-scale organised motions. In a flame, these differences influence the global strain rate, and so the heat losses due to flame radiation and thermal NO_x emissions. It is also shown that increased rates of mixing are not necessarily beneficial for a flame.

Introduction

George [1] deduced analytically that turbulent free shear flows such as jets and wakes can converge asymptotically to a variety of different self-preserving states, depending on their individual initial conditions. It has since become recognized that all turbulent flows are sensitive to the inlet and boundary conditions, even in the far field. For this reason the mixing characteristics of turbulent jets from different devices are anticipated to be individually distinctive and the greatest of care is required to reproduce two experiments, or to allow viable comparisons between experiments and models. However the extent to which given changes may influence the flow or a flame is still relatively poorly documented or understood.

In turbulent combustion, mixing is often the rate-limiting step. Knowledge of this has stimulated the development of a wide range of practical mixing devices, first with a view to increasing flame stability and combustion intensity e.g. swirl and bluff bodies, and later to reduce NO_x emissions, e.g. staged combustion. The rate-limiting importance of mixing is also the basis of physical modelling [52] and the first step in developing reliable mathematical and computational models. However, the interactions between turbulent mixing processes and combustion/chemical reactions are extremely complex. A wide range of chemical time-scales exist, from many gas-phase reactions that are typically faster than the mixing rates, to reactions such as those for soot formation, growth and oxidation, whose time-scale is typically longer than that of mixing. Hence the extent to which changes in initial conditions of a jet influence a flame is even more complex than on the flow alone.

Furthermore, accurate measurements, already difficult enough in cold-flow [53] are even much more difficult in flames. Consequently, many developments of turbulent combustion systems have to make use of both reacting and non-reacting investigations. This is particularly true in the systems that involve

highly unsteady flows, where the instantaneous flow differs dramatically from the mean flow, such as the precessing vortex core in swirling flows, e.g., [2].

A common target of most of the developments of "enhanced mixing" combustion devices has been to increase the rate of entrainment of surrounding air as indicated, for example, by spreading rate of these jets. This appears to be based on the widely held assumption that increased mean mixing rates are necessarily desirable, although this has not been adequately assessed. One such approach has been to stimulate, or excite, the large-scale, coherent motions in the emerging jet, based on the knowledge that such motions play a dominant role in the gross transport processes in jets and jet flames. Perhaps the best-known approach is the use of acoustic excitation, either in jets [3], jet flames [4] or in pulsed combustion systems [5]. Another approach is the use of mechanically oscillating devices, e.g. [6-7], and fluidically excited devices [8]. Yet, another class of mixing device is the fluidic devices that produce a jet of large-scale precession [9] or flapping [10].

Despite the large number of investigations of jet mixing devices, several important aspects remain poorly understood. Of these, the present paper seeks to address the following issues:

- The effect of initial conditions on jet's underlying turbulent structure and mixing behaviour,
- The near and far field flow and mixing behaviour in "excited" jets with highly unsteady initial flows,
- The implications of these differences in mixing on combustion performance.

Effects of subtle differences in initial conditions

Turbulent jets from round nozzles have been extensively studied for many decades. The three most common classes of round nozzle are a smoothly contracting nozzle, a sharp-edged orifice plate and a long pipe. Where the length of a supply pipe is sufficient, typically at least 70 diameters, the flow within it is fully developed. A jet with a fully-developed-pipe initial flow has a mean velocity profile that closely approximates the well-known 1/7 power law and an "M" shaped rms profile (Fig. 1a). Such jets are moderately common in burners because of their simplicity and ease of manufacture. In contrast, jets issuing from an aerodynamically well-designed smoothly contracting nozzle have an initial mean velocity profile of that is approximately uniform or of a "top-hat" shape (Fig. 1b). They also have a low and uniform rms, except at the very edge of the jet where the shear is high. Jets from these nozzles are widely studied because the uniform initial velocity profile is well suited to analytical (and some numerical) investigations. They also have a lower pressure drop than a long pipe because the supply pipe is of larger diameter. Sharp edged orifice plates are also simple to manufacture and are therefore widely used. The sudden contraction on the upstream side of the plate results in the well-known "vena contracta", where flow streamlines initially converge towards the jet axis. Their mean velocity is "saddle-backed" and the initial rms profile somewhere between those of the other two nozzles mentioned (Fig. 1c).

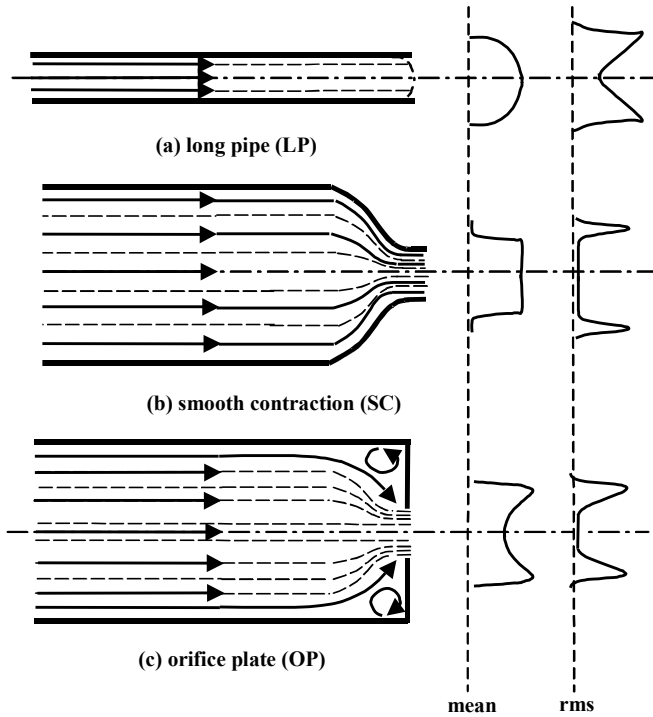


Fig. 1. Simplified representation of the initial velocity profiles of jets emerging from a long pipe, a smooth contraction and a sharp-edged orifice plate.

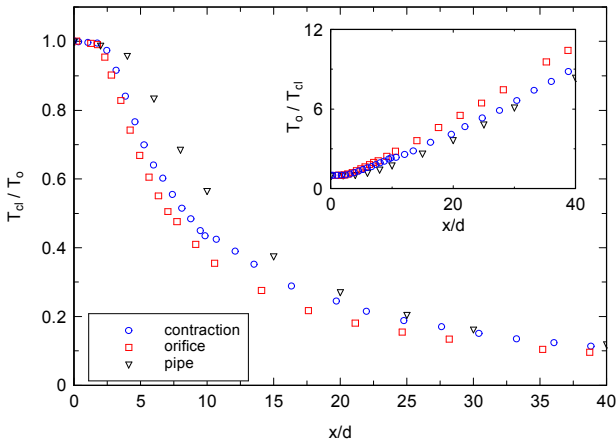


Fig. 2. Centreline variations of the mean scalar of the three jets [21].

The significance of initial conditions on the development of an axisymmetric jet-mixing layer near the nozzle exit has been well documented (e.g. [11-16]). However, until recently, they supported the classical belief that the influence of initial conditions of a flow decays rapidly with downstream distance to converge to a universal far-field flow with a fixed rate of spread and decay [17]. The classical view is that the differences in initial conditions result only in a shift in the location of the virtual origin of the jet (e.g. [18]), i.e. the “point” source in space from which the far-field mean flow emanates [19]. While this classical hypothesis was questioned analytically, e.g. by George [1], it has only recently been confirmed by experiments. Mi *et al.* [20-22] and Xu and Antonia [23] have shown that differences in initial conditions, as indicated by the exit velocity profiles, propagate throughout the entire field, affecting even the far-field spread rate, decay rate, and almost all turbulence statistics. The mean decay rate of the scalar fields of three jets of equal Reynolds number, Re , and diameter, but from different types of nozzles, is shown in Figure 2. It is clear that the decay rate for the orifice plate is the highest, followed by that from the smooth contraction

and then by that from the long pipe. Consistently, the rates of spread and decay of scalar advection are greatest in the orifice jet and lowest in the pipe jet (Fig. 3). The measurements also show that even the concept of a “virtual origin” of a classical jet is only an idealisation that is fundamentally flawed, since the virtual origin of the mean spreading rate is always different from that of the mean centre-line decay rate [20]. These values also depend upon the jet source conditions.

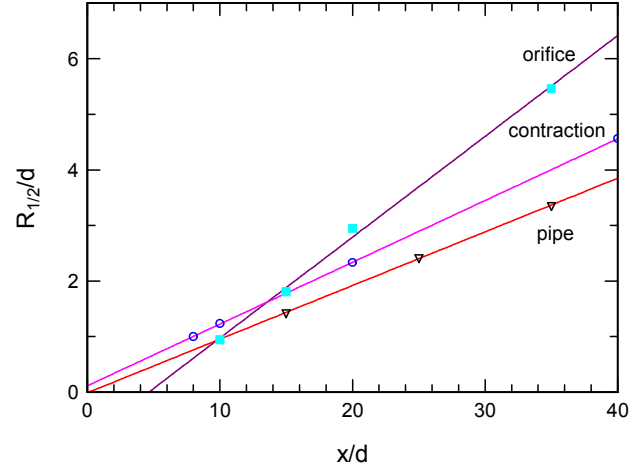


Fig. 3. Axial variations of the scalar half-radius of the three jets [21].

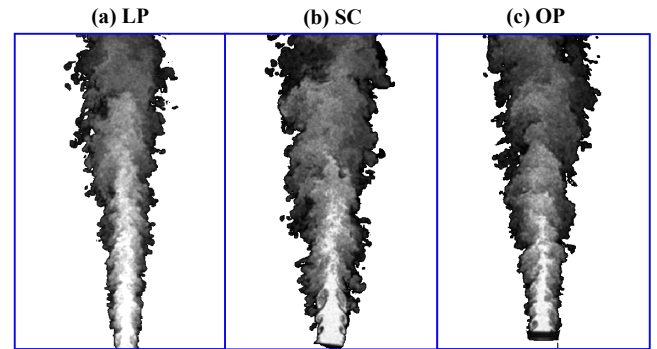


Fig. 4. Instantaneous planar Mie-scattering images of the scalar fields in (a) a LP jet, (b) a SC jet and (c) an OP jet [21].

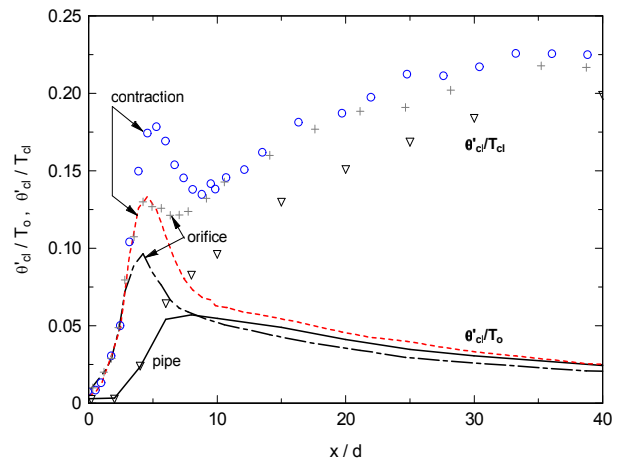


Fig. 5. The normalised centreline scalar RMS of jets from an orifice plate, a smooth contraction nozzle and a long pipe [21]. Here θ' is the rms of the fluctuations of the passive temperature marker, T_0 is the initial temperature difference between the jet and ambient fluid, and T_{cl} is the local mean temperature difference on the jet centre-line.

Mi *et al.* [21] further showed, using Mie scattering images of the concentration that, as might be expected, the differences in the scalar flow are associated with differences in the underlying flow

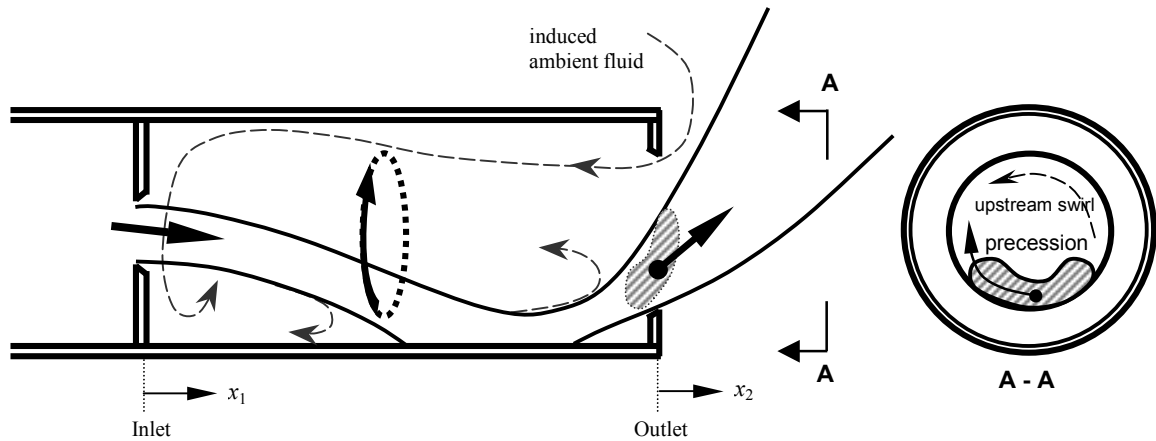


Fig. 6. A simplified schematic representation of the fluidic nozzle and the precessing jet flow [9].

structure (Fig. 4). This dependence is also reflected in the centreline variation of the scalar RMS (Fig. 5).

It should be noted that in these measurements the mixing of jet and ambient fluids was performed by slightly heating the jet relative to the ambient fluid, so providing a marker for the scalar. Here θ' is the rms of the fluctuations of the passive temperature marker, T_0 is the initial temperature difference between the jet and ambient fluid, and T_{cl} is the local mean temperature difference on the jet centre-line. In the near field, the locally normalised rms of fluctuations ($\langle \theta'^2 \rangle^{1/2} / \langle T \rangle_{cl}$) exhibits a local maximum slightly downstream from the potential core for the SC and OP jets, but not for the pipe jet. The presence of the maximum is associated with the convergence of the primary coherent vortex rings generated by rolling up the thin initial shear layer (see Fig. 4). The absence of the maximum for the pipe jet is attributed to the much weaker coherence in the underlying flow structures associated with initially the fully-developed pipe flow [20]. The second important difference is that the far-field, asymptotic values of the two jet flows are also different, with that from the pipe being lower. Based on previous studies, Mi et al. [20] hypothesised that the differences in the underlying coherent structures also exist in the far field. Taken together, these results demonstrate that the far field of a jet does not forget its origin entirely. Given these differences in both the mean flow everywhere and especially in the initial flow where a lifted flame is stabilised, differences in a flame might also be expected, as discussed below.

Effects of highly unsteady initial flow on jet mixing

Precessing jets (PJ) are a class of highly unsteady flows which are of both scientific interest and practical significance because of the benefits found when used as industrial burners. Precession is the term used to describe the azimuthal oscillation of a flow about an axis. Examples in fluid mechanics include the precessing vortex core found in swirling flows [2] and precessing jet flows [9]. The former precession in swirl burners can have significance in the well-known combustion driven oscillations in gas turbine combustors.

Precessing jet flows have found application in rotary kilns where high radiant heat and low NO_x emissions are sought [24-25]. Direct comparison of the flames from a PJ nozzle and an optimized high momentum jet burner in a pilot-scale cement kiln simulator demonstrated a net increase in heat transfer of 4% and reduction in NO_x emissions by 30% [26]. These precessing flows can be generated naturally in an axisymmetric fluidic device [9,27] or by mechanical rotation of a nozzle device [28-29]. The registered trade name for the burners that utilise the fluidic PJ nozzle [30] is Gyro-Therm[®].

The unsteady flow within and emerging from the fluidic PJ nozzle is illustrated schematically in Fig. 6. The dimensions of the chamber are such that the instantaneous jet reattaches asymmetrically within it and emerges from the chamber outlet at about 45° to the nozzle axis. The asymmetry is accompanied by a rotating pressure field so that the entire flow-field, including the emerging jet, precesses [9]. The flow within the chamber is complex, containing a large-scale reverse flow zone and a region of high swirl at the upstream end of the chamber. The frequency of the precession is two orders of magnitude lower than that of formation of the primary vortices in the SC free jet mentioned above (see Fig. 4b).

However, of particular interest to the present discussion, the precession of the emerging asymmetric jet causes a large increase in the initial spreading rate of the time-averaged jet relative to a “steady” jet, as clearly demonstrated by the concentration half-width contours of the FPJ flows in Fig. 7. An increase in initial spreading rate is not unique to the PJ nozzle. Alternative devices which have also achieved increased spreading include a fluidic device [8], mechanical devices [6] and acoustic devices [3, 31]. The increased initial spread led those authors to refer to their respective devices as “enhanced mixing” nozzles, under the assumption that increased spreading implies increased entrainment, and that increased entrainment implies enhanced mixing. However, while the arguments sound plausible, they may not necessarily be correct, at least for highly unsteady jets.

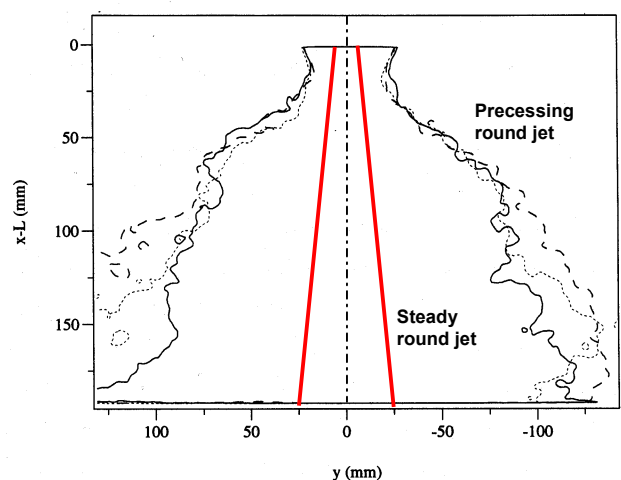


Fig. 7. Concentration half-width contours of the FPJ flows. The jet initial diameter is 7.3 mm [33]. —, $\text{Re} = 37,000$; - - - -, $\text{Re} = 49,200$; ·····, $\text{Re} = 61,500$.

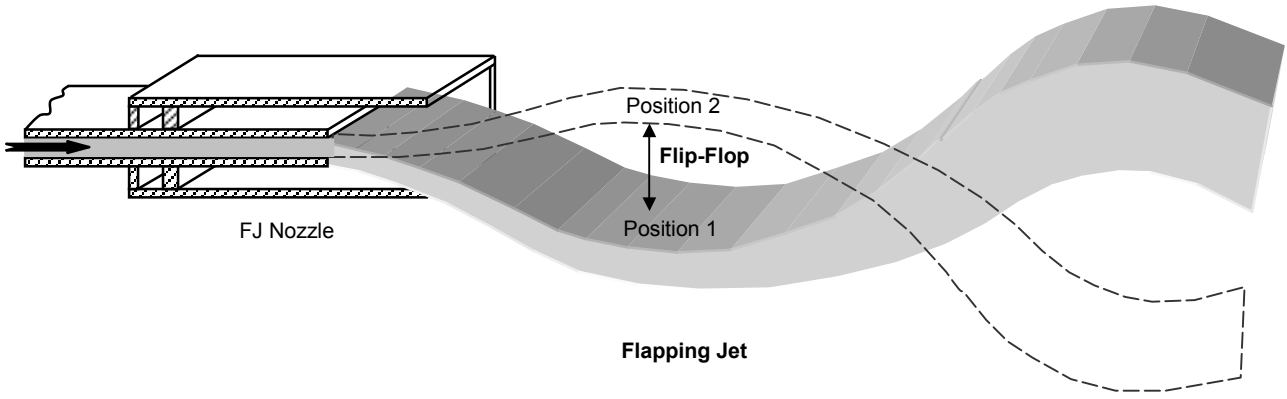


Fig. 8. A simplified schematic representation of the fluidic nozzle producing a pseudo two-dimensional flapping motion.

Mi and Nathan [10] used the fluidic device shown in Fig. 8 to generate a two-dimensional flapping jet that is broadly analogous to the azimuthal precession motion. The chamber of this device is rectangular in cross-section, and the inlet nozzle is of smaller span than the chamber to provide a feed-back path and allow the pressure fields on either side of the jet to communicate. Their flow visualization and velocity measurements showed that this jet also produces a significant increase in the initial spreading rate of the jet [10]. The *initial rate* of entrainment outside the chamber is also higher, as shown by the volume flux measurements through various downstream cross-sections (Fig. 9). However, the *total* amount of ambient fluid entrained by the flapping jet was found to be less than that by the non-flapping counterpart (Fig. 9).

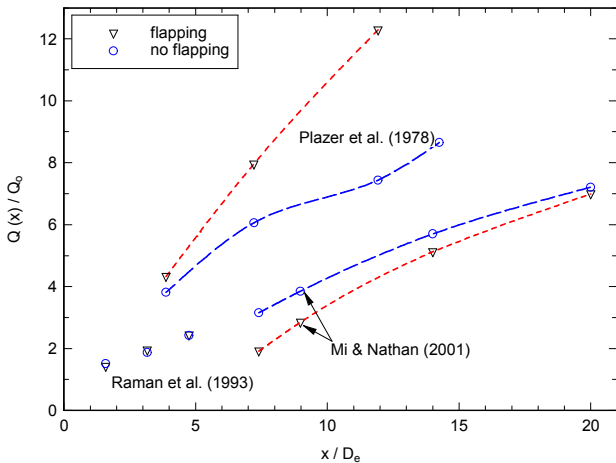


Fig. 9. Entrainment of the flapping jet relative to that of a steady jet [10].

Figure 9 presents a three-dimensional integral of the axial velocity flux through different transverse planes obtained in [10]. It is important to note that the axial coordinate is measured from the inlet plane of the nozzle chamber. This provides a direct comparison of the volume flux of fluid for the cases with the nozzle chamber present and removed. The volume flux is also normalized relative to the flow introduced through the nozzle. It shows that the initial *rate* of entrainment downstream from the chamber exit is greater for the flapping jet than the steady jet, consistent with the increased rate of spread resulting from the flapping motion. Nevertheless, the total volume flux for the flapping jet never actually reaches that of the steady jet counterpart. This is because the presence of the chamber walls inhibits the jet entrainment of ambient fluid from outside the chamber. That the presence of the nozzle chamber creates a net loss of entrainment is perhaps not unexpected given the fact that the chamber creates a pressure loss and the second law of thermodynamics. The mechanical flapping nozzle (no chamber) of Plazer et al. [7] was measured to produce a jet with significantly more ambient fluid entrained (Fig. 9). However this

measurement was only performed along one axis, so the finding relies on the assumption of two-dimensionality which is not necessarily correct.

We have also conducted scalar measurements for unsteady oscillating jets. Newbold [33] measured the concentration field of an unconfined precessing jet from the fluidic nozzle (FPJ). Parham [34] studied the effect of a co-flow and confinement on the same flow, while Nobes [35] measured the concentration field of a precessing jet from a mechanically rotating nozzle. The mechanical nozzle, shown in Fig. 10 and described in detail elsewhere [36], can provide well-defined and controllable initial conditions for the mechanical precessing jet (MPJ). One important finding of the work on the MPJ flow is the importance of the dimensionless frequency of precession, the precession Strouhal number, $St_p = f_p d / u_e$. Here f_p is the frequency of precession, d the nozzle exit diameter and u_e the bulk-mean exit velocity. As St_p approaches zero, the precession has negligible influence on the flow, and its trajectory remains at the exit angle. However, above a critical Strouhal number, St_c , precession causes the jet to “spiral” into a helix [28,29]. For $St_p > 0.01$, the helix converges upon itself within about 5 nozzle diameters from the exit plane [29]. This is associated with a low-pressure core associated with the asymmetric entrainment [36]. Figure 13 compares the average scalar mixing field of a non-

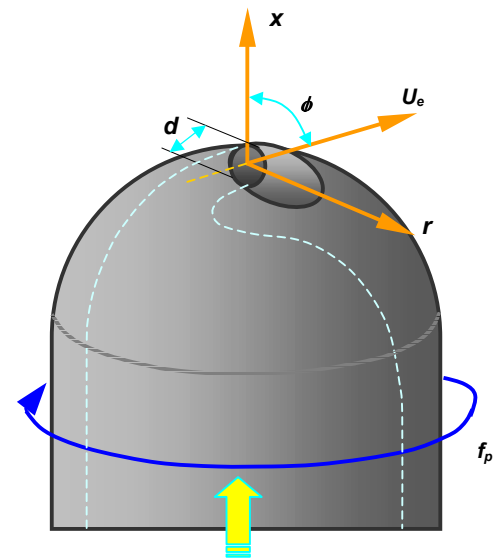


Fig. 10. Schematic representation of the MPJ nozzle that produces a PJ with well-defined and controllable initial conditions [27].

precessing round jet and the phase-averaged scalar field of the MPJ above St_c . The laser sheet cuts through the helix, which is evident for approximately one full turn. Downstream from the helix, the global jet undergoes a transition to a spreading rate

broadly comparable with that of a simple jet. Hence the rapid initial spreading rate does not extend into the far field (Fig. 13). The precession motion also decays through the transition region, so that the phase-averaged scalar field is axi-symmetric for $x/d > 15$ (Fig. 13). In addition, frequency spectra reveal that neither the precession, nor any sub-harmonic, is evident beyond a downstream distance of about 12-15 nozzle diameters [29]. The near-field flow from the FPJ nozzle does differ from that of the MPJ in that it does not transcribe a clear helical trajectory. The initial structure is also highly non-uniform and more complex [32]. However a similar decay in precession is supported by the instantaneous images, which do not reveal any correlation between far-field structure and the position of the emerging jet.

Comparison of the instantaneous concentration measurements of the MPJ (Fig. 11) and FPJ (Fig. 12) suggests that, while there are significant differences in the details of the flow, especially in the near field, many of the gross features are similar. Importantly, both jets exhibit a rapid initial spreading followed by the convergence to a far-field flow. Likewise, broad features of their flames are similar [41].

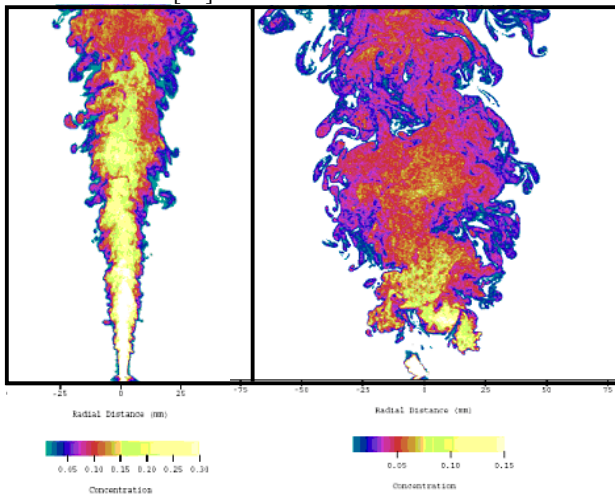


Fig. 11. The instantaneous non-reacting mixture fraction in a simple jet (left) and a mechanically precessing jet with $St = 0.0126$ (right). The jet initial diameter is 3 mm and $Re = 3,800$ [35].

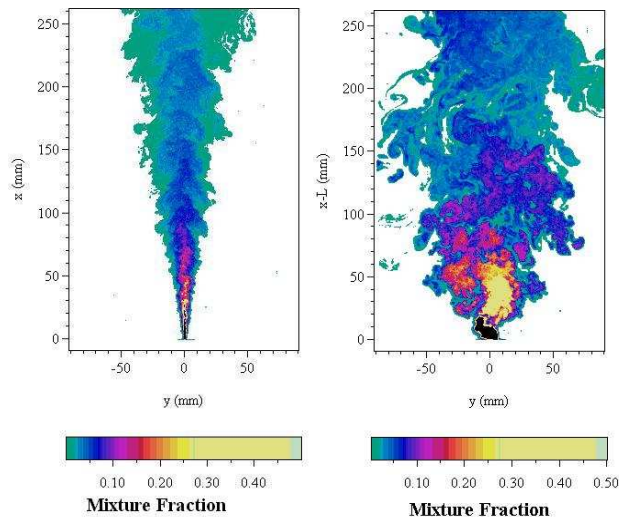


Fig. 12. Instantaneous non-reacting mixture fraction of the emerging simple jet (left) and a fluidic precessing jet (bottom). The jet initial diameter is 3 mm and $Re = 20,000$ [33].

Figure 14 shows that the local phase-averaged maximum velocity, $\langle U_m \rangle$, of the “instantaneous” precessing jet flow in the near field ($x/d < 15$), exhibits a substantially stronger decay than the equivalent, $\langle U_c \rangle$, of the non-precessing jet. This is consistent with the precession causing an increase in the strain on the jet.

Consistently, the conditionally averaged half-width, $Y_{1/2}$, of the local precessing jet flows spreads more rapidly than does that of the half radius, $R_{1/2}$, of the non-precessing round jet (Fig. 15). Taken together, this implies that the precession of the entire jet promotes the *initial* entrainment of ambient fluid, consistent with the flapping jet discussed above. Figs. 14 and 15 also suggest that the initial velocity decay and spread rates of the precessing jet increase as the Strouhal number St_p increases. However, in the far field, the strain rates in the flows for $St > St_c$ are reduced, as determined by two point spatial correlation contours of the scalar field for both the MPJ [35] and FPJ [33] flows.

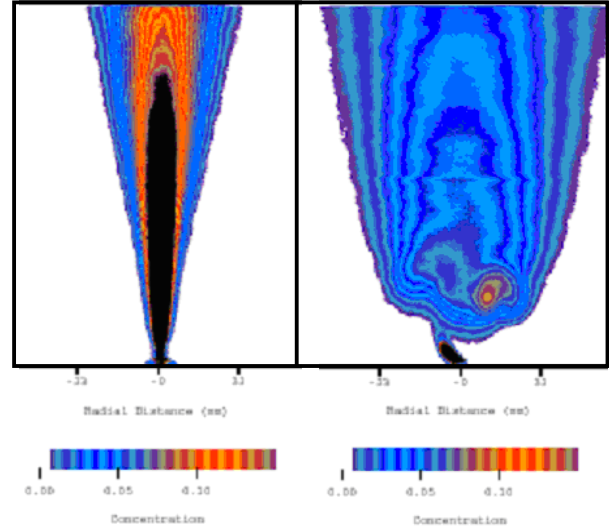


Fig. 13. Mean non-reacting mixture fractions of a non-precessing jet (left) and a MPJ with $St = 0.0096$ (right). The jet initial diameter is 3 mm and $Re = 3,800$ [34].

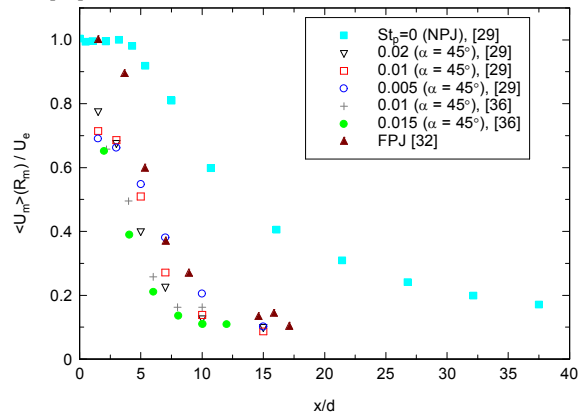


Fig. 14. Axial variations of local maxima of the conditionally averaged (“instantaneous”) precessing jet, $\langle U_m \rangle(R_m)$ from the MPJ nozzle and the centreline $\langle U_c \rangle$ decay for the non-precessing jet ($\alpha = 0^\circ$) [29].

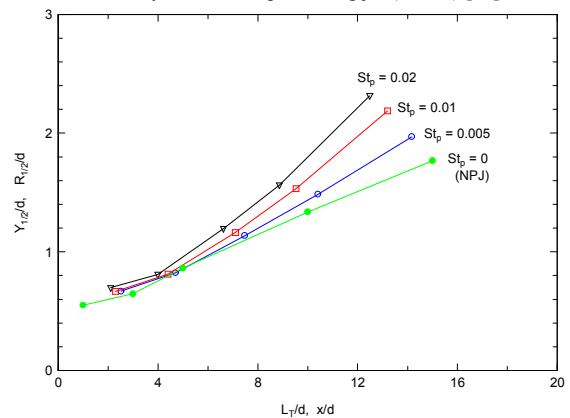


Fig. 15. Axial variations of the averaged half-width $Y_{1/2}$ for the MPJ and the non-precessing jet ($\alpha = 0^\circ$) [29].

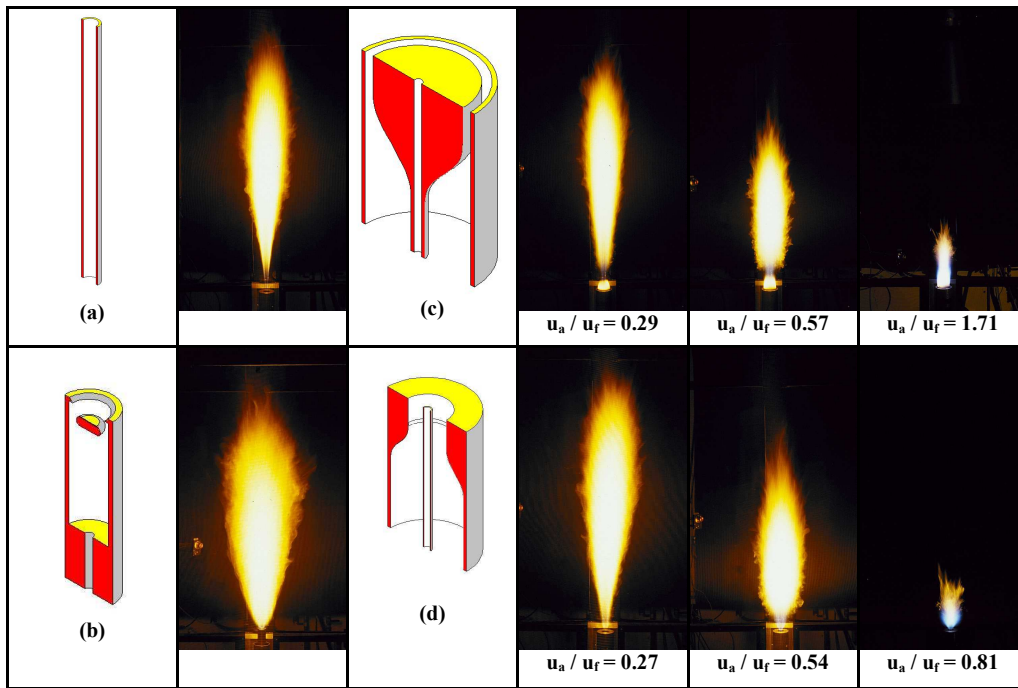


Fig. 16. Time-averaged flames from (a) an axial jet nozzle, (b) a precessing jet nozzle, (c) a bluff-body nozzle, and (d) a swirling jet nozzle. All nozzles have the same central fuel pipe, are fired with propane and have identical fuel velocity, u_f , equating to $Re_f = 20,000$ and are presented to scale [40].

Effects of initial conditions on flames

The non-linear nature of flames means that they can be highly sensitive to initial conditions. For example, Dahm and Dibble [59] have shown both experimentally and theoretically that a co-flow velocity of the order of only 1% of the jet velocity leads to a reduction of the order of 50% in the blow out velocity compared with stagnant air. Likewise, a slight co-flow of the order of 2% has a dramatic effect on the length of pulsed flames [60]. However other aspects of initial and boundary conditions, such as the effect of initial velocity profile, have not been considered previously. Even the measurements of basic properties such as lift-off height and blow-off velocity as reported in text books [e.g. 54] do not raise the issue. Data is only presented for a single nozzle type (a long pipe), based on the pioneering measurements of Kalghatgi [55], and the lack of reference to possible effects of initial conditions evokes the tacit assumption that performance is independent of the nozzle type. However, our recent measurements [56] have shown that lift-off and blow-off velocities are 40% and 17% higher, respectively, for a smooth contraction than a long pipe, the asymptotic flame length of the smooth contraction is 13% greater and the radiant energy from the smooth contraction nozzle is lower.

A broader study of the effect of more significant changes to mixing on global flame performance was performed by Newbold *et al.* [40]. They compared the flames from four nozzles with dramatically different mixing conditions: a simple jet issuing from a long pipe, a PJ nozzle, a swirl jet and a bluff body jet. The flames were unconfined to avoid the influences of confinement, which can also be significant, and examined in with identical facilities to avoid subtle differences in conditions. The four burners were carefully designed to utilise the identical source conditions, including fuel nozzle geometry, (for the PJ nozzle this corresponds to the inlet to the nozzle chamber) and the same fuel flow rate. Each of these flames, as shown in Fig. 16, are dramatically different. However, before returning to a detailed

comparison of each, we will first discuss the key features of precessing jet flames, which are least well known.

When firing gas in the range $St > St_c$, the PJ flame is typically stabilised several nozzle diameters downstream from the burner. However the flame length is several hundred times the nozzle diameter. Hence nearly all of the combustion occurs *downstream* from the near-field region where precession is evident. Various investigations have confirmed that precession is also not evident for $St > St_c$, which is also the range in which the fluidic PJ nozzle operates [27]. Newbold *et al.* [37] identified and analysed the large-scale structures that propagate through the flame using the “volume rendering” technique of Mungal *et al.* [38]. This is constructed from a time-series of images of the edge of the flame, as determined from the visible light naturally emitted by it. They showed that the frequency of these large-scale motions is more than an order of magnitude lower than the precession frequency. Instead, in an open-flame environment, these large-scale motions are driven by buoyancy, while in a kiln they are driven by the confined, co-flowing environment. The independence from the precession frequency of the large-scale motions within the PJ flame is further supported by phase-averaged images of the OH radical excited by laser-induced fluorescence [39].

Although there seems to be no direct correlation between a PJ flame itself and the precession, the effect of precession within the upstream flow produces a dramatic influence on the flame. The rapid initial spreading produces a flame that is typically three times wider than the equivalent non-precessing axial jet flame with the same fuel and flow rate, although the length of the flame is only slightly shorter [40]. This results in a net increase in volume. Note again that the global characteristics of the flames from the MPJ and FPJ nozzles are similar, provided that the Strouhal number of precession is comparable [41].

The global mixing residence time of the fuel gases within a flame, τ_G , can be defined as the flame volume divided by the volume flow-rate of fuel [42]. On this basis, Newbold *et al.* [40] compared the global mixing rate the four burner types shown in Fig. 16. Both the swirling and bluff body flows act to increase global mixing rates and flame strain relative to a simple jet, as evidenced by a reduced flame volume relative to the simple jet. In contrast, the PJ flame acts to decrease the global mixing rate and flame strain, which is related to the global strain rate defined by Rokke (1992 & 1994), as evidenced by an increased flame volume. Using an independent measurement of flame strain, also based on the volume rendering technique, Newbold *et al.* [43] found that PJ flames have a global flame strain that is an order of magnitude lower than that of a simple jet flame. This is consistent with the reduced far-field strain found in non-reacting measurements described above.

Flame strain rate has a dramatic effect on soot formation and flame radiation. This is because, unlike the primary reactions in a flame, the time-scales for the processes of soot formation, growth and oxidation are of the same order as the time-scales of mixing. The pioneering study by Kent and Bastin [44] shows that the soot volume fraction in a turbulent diffusion flame increases with decreased global strain, defined as u/d at the source. The same trend is also found by numerous fundamental studies of local flame strain in laminar flames. At strain rates below the soot-limiting critical strain rate, soot concentration decreases with increasing strain rate [45]. Decroix and Roberts [46] also found that the width of the soot field in a laminar counter-flow diffusion flame decreases linearly with the square root of the local strain rate. Our measurements have confirmed the trend in turbulent flames. The reduced strain in the far-field of PJ flames results in increased local soot volume fraction within the reaction zones and in three to six times more soot within comparable regions of the simple jet (SJ) flame [47]. The soot volume fractions within the bluff body (BB) flame are slightly lower, while the total soot within it is more than an order of magnitude lower [47]. It is important to make a distinction between the desirable presence of soot within a flame and the undesirable presence of soot emitted from a flame. Since the soot is consumed within the PJ flame envelope, its presence constitutes neither a loss of combustion efficiency nor an environmental threat.

The presence of soot within a flame acts to increase the flame emissivity. As solid particles, soot radiates incandescently over a wide range of wavelengths (i.e. broad-band), so radiating more effectively the narrow-band radiation from molecular processes. For this reason, lowering flame strain acts to promote flame radiation, both by increasing flame volume and by increasing the amount of soot within the flame [47], as described above. The effect of changing flame volume on flame radiation is shown in Fig. 17, where the radiant fraction, χ_r , is defined as the percentage of the total energy of the flame that is released by radiation [40]. Perhaps surprisingly, the relationship is approximately linear across this wide range of flames spanning four different types of burners. Since the heat losses from a flame are typically dominated by radiation, this implies that the mean flame volume has a controlling influence on temperature for these flames. Flame radiation controls thermal NO_x emissions from simple jet turbulent diffusion flames through its effect on flame temperature [42]. Newbold *et al.* [40] therefore concluded that the global flame strain, through its effect on radiation, has a controlling influence on thermal NO_x emissions. The significance of this finding, in the context of modelling, is that the accurate prediction of mean flame volume and strain is of first order importance in predicting flame temperature, and hence, thermal NO_x emissions, again highlighting the importance of mixing.

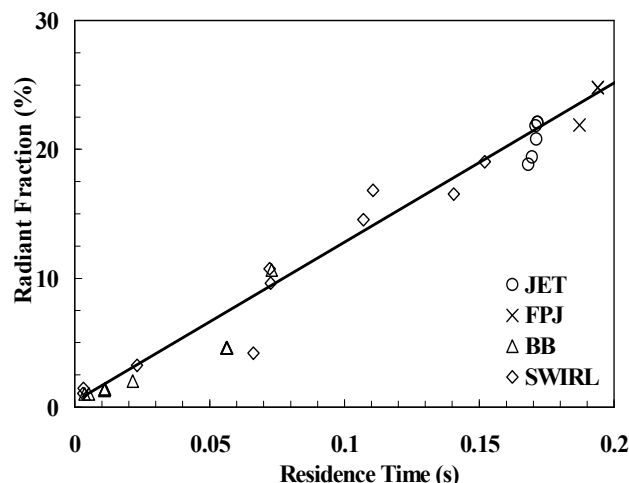


Fig. 17. The relationship between radiant fraction and global residence time for all of the flames in Fig. 16 [40].

In gaseous jet flames, the precessing flows with $St > St_p$ result in lower global strain, and so, increased radiant heat transfer and lower thermal NO_x emissions than simple jet, swirling jet and bluff-body jet flames [40]. This is further demonstrated by Pilot scale measurements in a cement kiln simulator which demonstrated that, relative to an optimised high momentum burner, the fluidic PJ flow provides about 4% increase in radiant heat-transfer and a shift in the profile toward the burner. Those measurements also revealed an equivalent reduction in NO_x emissions, when corrected for differences in heat transfer, of about 30% [26]. These measurements are consistent with full-scale plant data. In natural-gas-fired cement [47] and lime [48] kilns, the precessing jet nozzle is found to typically provide a reduction in specific fuel consumption and/or increase in output by 5 to 10% and a reduction in NO_x emissions by 30-50%. This reduction is significantly higher than the 5-10% difference at ambient conditions because the 800-1100°C air temperature in a rotary kiln means that NO_x production is dominated by the thermal route, while prompt NO_x is also significant at ambient temperature. The high temperatures in a kiln also increase the burn-out of any residual soot.

Similar trends are found to apply with the combustion of pulverised coal in cement kilns [49]. However, the combustion of solid fuels is more complex than that of gas. Unsteady effects are also significant, with precession enhancing the non-uniform distribution of particles, termed "clustering" [50].

Conclusions

That differences in the initial flow from a jet, due to nozzle profile or co-flow for example, influence the downstream flow and flame is well established. However, the detailed nature, extent and underlying causes of these influences are still an area of active investigation. The issues which the present review has addressed are as follows. Firstly, it is clear that even subtle differences in the initial flow of a non-reacting flow do propagate into the far field, so that a jet never entirely forgets its origin. It is also evident that these differences relate to differences in the underlying flow structure, although the details of this remain to be resolved. This finding contradicts the classical belief that initial conditions influence only the near field and can be accounted for by a shift in the virtual origin. On the other hand, even with the introduction of dramatic differences to the initial flow, such as by precession of the entire jet at sufficiently high Strouhal numbers, the far-field flow may still converge to a flow which is broadly comparable with that of a simple jet. Hence, the classical belief appears to be true to the first order. At present

there is insufficient information to put bounds on the maximum and minimum rates of spread, decay and normalised fluctuations that can result from differences in initial conditions.

Secondly, the relationship between initial spreading rates and overall mixing is more complex than is often assumed. Those nozzles which produce a naturally occurring large-scale oscillation, either two-dimensional flapping or precession, do produce a large increase in the mean initial spreading and, with this, an increase in the initial rate of entrainment and scalar mixing. However, because of the energy losses within the nozzle itself, these devices may decrease the total entrainment or mixing relative to a simple jet. Also the far-field rates can be quite different from the near-field. Thus the total entrainment of a flapping jet from a fluidic device is less than that for the steady jet when the length of the nozzle chamber is accounted for [10]. Similarly the flame volume of both the fluidic [40] and mechanical [41] precessing jet nozzles are significantly larger than that of the steady jet counterpart with identical nozzle diameter, fuel and flow rate. Since the flame volume is a direct measure of the volume required to mix the fuel to the stoichiometric contour, the total mixing rate of the precessing flow is reduced. Hence the reduced overall mixing rate of the flame is broadly consistent with cold-flow measurements.

However, the finding which is arguably least well recognised is that there is no direct correlation between increased mean mixing rates and the “desirability” of flame performance. Despite the fact that precessing jet nozzles reduce the net mixing rate of a jet and jet flame, they can nevertheless provide significant benefits for those applications where high radiation is desirable. This is because radiation from gas flames is dominated by the contribution of soot, where it is present, since soot produces broadband, incandescent radiation while non-sooting flames only produce narrow-band radiation. The production of soot, in turn, is favoured by reduced strain rates. Hence low strain flames can be desirable, so long as the soot is burned out within the flame envelope. It should also be noted that, while in principle it is possible to produce low-strain rate flames by other means (e.g. by increasing the diameter of a nozzle), this is difficult to achieve in practice without increasing the flame length, which usually a constraining parameter in design.

For these reasons researchers in fluid-mechanics and combustion should take the greatest of care to ensure that initial and boundary conditions are well defined and fully specified. Care should also be exercised in use of the terms “enhanced mixing” or “better mixing”. They should not be as a synonym for increased mixing rates or without specifying how they are better, since some aspects of combustion benefit from reduced mixing rates.

Acknowledgments

The present paper summarises research which has been undertaken over many years, predominantly with support of the Australian Research Council and FCT-Combustion Pty Ltd. The work has been undertaken collaboratively and the authors also wish to acknowledge that many colleagues, whose work is referenced, have contributed to the development of the ideas expressed here.

References

[1] George, W.K., *Recent Advances in Turbulence* (eds. Arndt, R.E.A. & George, W.K.), Hemisphere, New York, 1989, pp.39-73.
 [2] Syred, N., and Beer, J.M., Combustion in Swirling Flow: A Review, *Combust. & Flame*, **23**, 1974, 143-201.
 [3] Hill, W.G. Jr. and Greene, P.R., Increased Turbulent Jet Mixing Rates Obtained by Self Excited Acoustic Oscillations, *J. Fluids Engineering*, **99**, 1977, 520-525.

[4] Gutmark, E., Parr, T.P., Hanson-Parr, D.M. and Schadow, K.C., On the role of large and small-scale structures in combustion control, *Combust. Sci. & Tech.*, **66**, 1989, 107-126.
 [5] Candel, S.M. (1992), “Combustion Instabilities Coupled by Pressure Waves and Their Active Control”, *Proc. Combustion Institute*, **24**, 1277-1296.
 [6] Simmons, J.M., Lai, J.C.S. and Platzer, M.F., Jet Excitation by an Oscillating Vane, *AIAA J.*, **19**, 1981, 673-676.
 [7] Platzer, M. F., Simmons, J. M. and Bremhorst, K., Entrainment characteristics of unsteady subsonic jets, *AIAA J.*, **16**, 1978, 282-284.
 [8] Viets, H., Flip-flop jet nozzle. *AIAA J.*, **13**, 1975, 1375-1379.
 [9] Nathan, G.J., Hill, S.J. and Luxton, R.E., An axisymmetric fluidic nozzle to generate jet precession, *J. Fluid Mech.*, **370**, 1998, 347-380.
 [10] Mi, J., and Nathan, G.J., Mixing characteristics of a flapping jet from a self-exciting nozzle, *Flow, Turb. & Combust.*, **67**, 2001, 1-23.
 [11] Bradshaw, P., The effect of initial conditions on the development of a free shear layer. *J. Fluid Mech.*, **26**, 1966, 225-236.
 [12] Flora, J.J. and Goldschmidt, V.M. *AIAA J.*, **7**, 1969, 2344-2346.
 [13] Hussain, F. & Clark, A.R. On the coherent structure of the axisymmetric mixing layer: a flow-visualization study, *J. Fluid Mech.*, **104**, 1981, 263-294.
 [14] Husain, D.Z. & Hussain, F., Axisymmetric mixing layer: influence of the initial and boundary conditions, *AIAA J.*, **17**, 1979, 48.
 [15] Yule, A.J. Large-scale structure in the mixing layer of a round jet. *J. Fluid Mech.*, **89**, 1978, 412-432.
 [16] Zaman, K. B. M. Q. & HUSSAIN, A. K. M. F., Natural large-scale structures in the axisymmetric mixing layer, *J. Fluid Mech.*, **138**, 1984, 325-351.
 [17] Richards, C.D. & Pitts, W.M., Global density effects on the self-preservation behaviour of turbulent free jets, *J. Fluid Mech.*, **245**, 1993, 417-435.
 [18] Townsend, A.A., *The Structure of Turbulent Shear Flow*. 2nd edition, 1976, Cambridge University Press.
 [19] Chen, C.J. & Rodi, W. *Vertical Turbulent Buoyant Jets – A Review of Experimental Data*. 1980, Pergamon.
 [20] Mi, J., Nobes, D.S. and Nathan, G.J., Influence of jet exit conditions on the passive scalar field of an axisymmetric free jet, *J. Fluid Mech.*, **432**, 2001, 91-125.
 [21] Mi, J., Nathan, G.J. and Nobes, D.S., Mixing characteristics of axisymmetric free jets from a contoured nozzle, an orifice plate and a pipe, *J. Fluid Eng., Trans ASME*, **123**, 2001, 878-883.
 [22] Mi, J. and Nathan, G.J., Momentum mixing characteristics of turbulent axisymmetric jets with different initial velocity profiles, to be submitted for *J. Fluid Mech.*
 [23] Xu, G. and Antonia, R. A., Effect of different initial conditions on a turbulent round free jet, *Expts. Fluids*, **33**, 2002, 677-683.
 [24] Manias, C.G. and Nathan, G.J., The Precessing Jet Gas Burner - A Low NO_x Burner Providing Process Efficiency and Product Quality Improvements, *World Cement*, March, 1993, 4 -11.
 [25] Manias, C.G. and Nathan, G.J., Low NO_x clinker production, *World Cement*, May, 1994, 21-26.
 [26] Parham, J.J., Nathan, G.J., Smart, J.P., Hill, S.J. and Jenkins, B.G., The relationship between heat flux and NO_x emissions in gas fired rotary kilns, *J. Inst. Energy*, **73**, 2000, 25-34.
 [27] Mi, J. and Nathan, G.J. Self-excited Jet precession Strouhal Number and its influence on turbulent mixing characteristics, *J. Fluids & Structures*, **19**, 2004, 851-862.
 [28] Schneider, G.M., Froud, D., Syred, N., Nathan, G.J. and Luxton, R.E., Velocity Measurements in a Precessing Jet Flow using a Three Dimensional LDA System, *Expts. Fluids*, **23**, 1997, 89-98.
 [29] Mi, J., and Nathan, G.J. Statistical analysis of the velocity field in a mechanical precessing jet flow, *Phys. Fluids*, **17**(1), 2005, in press.
 [30] Luxton, R. E. and Nathan G. J., Mixing using a fluid jet, *Patent Application No PI4068/87*, Australian Patent Office, 1987.
 [31] Abell, C.J., Acoustic coupling in a turbulent flow, *Proc. 6th Australasian Hydr. & Fluid Mech. Conf.* (Adelaide), 1977, pp41-45.
 [32] Wong C.Y. Lanspeary P.V. Nathan G.J., Kelso, R.M. & O’Doherty, T., Phase-averaged velocity in a fluidic precessing jet nozzle and in its near external field, *Exp. Therm. Fluid Sci.*, **27**, 2003, 515.
 [33] Newbold, G.J.R., *PhD Thesis*, 1997, Department of Mechanical Engineering, The University of Adelaide.
 [34] Parham, J.J., *PhD Thesis*, 2000, Department of Mechanical Engineering, The University of Adelaide.
 [35] Nobes, D.S., *PhD Thesis*, 1998, Department of Mechanical Engineering, The University of Adelaide.

- [36] Schneider, G.M., *PhD Thesis*, 1996, Department of Mechanical Engineering, The University of Adelaide.
- [37] Newbold, G.J.R., Nathan, G.J., and Luxton, R.E., The Large Scale Dynamic Behaviour of an Unconfined Precessing Jet Flame, *Combust. Sci. and Technol.*, **126**, 1997, 71-95.
- [38] Mungal, M.G., Karasso, P.S. and Lozano, A., The visible structure of turbulent jet diffusion: Large-scale organisation and flame tip oscillation, *Comb. Sci. Tech.* **76**, 1991, 165-185.
- [39] Reppel, J., *PhD Thesis*, 2003, Department of Chemical Engineering, The University of Adelaide.
- [40] Newbold, G.J.R., Nathan, G.J., Nobes, D.S. and Turns, S.R., Measurement and prediction of NO_x emissions from unconfined propane flames from turbulent-jet, bluff-body, swirl and precessing jet burners, *Proc. Combust. Inst.* **28**, 2000, 481-487.
- [41] Nathan, G.J., Turns, S.R. and Bandaru, R.V., The influence of jet precession on NO_x emissions and radiation from turbulent flames, *Comb. Sci. Tech.*, **112**, 1996, 211-230.
- [42] Turns, S.R., and Myhr, F.H., *Combust. Flame* **87**, 1991, 319-335.
- [43] Newbold, G.J.R. and Nathan, G.J., The influence of changes to mixing on the sooting and NO_x emission characteristics of unconfined turbulent jet diffusion flames, *Develop. Chem. Eng. & Min. Proc.* **7**, 1999, 361 – 374.
- [44] Kent, J. H. & Bastin, S. J., Parametric effect on sooting in turbulent acetylene diffusion flames, *Comb. & Flame* **56**, 1984, 29-42.
- [45] Vandsburger, I. M., Kennedy, I. M. and Glassman, I., Sooting counter-flow diffusion flames with varying velocity gradients” *Proc. Combust. Inst.* **20**, 1984, 1105-1112.
- [46] Decroix, M. E. & Roberts, W. L., Transient flow field effects on soot volume fraction in diffusion flames, *Comb. Sci. & Tech.* **160**, 2000, 165-189.
- [47] Qamar N.H., Nathan, G.J., Alwahabi, Z.T., and King, K.D., The effect of global mixing on soot volume fraction: Measurements in simple Jet, precessing jet and bluff body flames, *Proc. Combust. Inst.* **30**, 2004, to appear.
- [48] Videgar, R., Gyro-therm technology solves burner problems, *World Cement*, November, 1997.
- [49] Manias, C.G. Balendra, A.S. and Retallack, D.J., New combustion technology for lime production, *World Cement*, December, 1996.
- [50] Nathan, G.J. and Hill, S.J., Full scale assessment of the influence of a precessing jet of air on the Performance of pulverised coal flame in a cement kiln, *Proc. 6th Euro. Conf. Ind. Furn. & Boilers* (Eds: Reis, Ward & Leuckel), v. 1, 2002, pp 155-168.
- [51] Smith, N.L., Nathan, G.J., Zhang, D.-K. and Nobes, D.S., The Significance of Particle Clusters in Pulverised Coal Flames, *Proc. Combust. Inst.* **29**, 2002, 797-804.
- [52] Rhine, J.M. and Tucker, R.J., *Modelling of Gas-Fired Furnaces and Boilers*, 1991, McGraw Hill.
- [53] Mi J. and Nathan G.J., The influence of probe resolution on the measurement of a passive scalar and its derivatives, *Expts. Fluids*, **34**, 2003, 687-696.
- [54] Turns, S. R., *An Introduction to Combustion; Concepts and Applications*, 2nd Ed., 2000, McGraw-Hill.
- [55] Kalghatgi G.T., Blow-out stability of gaseous jet diffusion flames. Part I: In Still Air, *Combust. Sci. & Technol.*, **26**, 1981, 233-239.
- [56] Langman, A.S., Nathan, G.J. and Ashman, P.J., A study of the global differences between axisymmetric turbulent free jet flames from a smooth contraction and a pipe with well defined boundary conditions, *15th Australasian Fluid Mechanics Conference*, 13-17 Dec, 2004, *The University of Sydney*.
- [57] Røkke, N.A., Hustad, J.E., Sønju, O.K., and Williams, F.A., *Proc. Combustion Institute*, **24**, 1992, 385-393.
- [58] Røkke, N.A., Hustad, J.E., and Sønju, O.K., *Combust. Flame* **97**, 1994, 88-106.
- [59] Dahm, W.J.A. and Dibble, R.W. Coflowing turbulent jet diffusion flame blowout, *Proc. Combust. Inst.*, **22**, 1988, 801-808.
- [60] Hermanson, J.C., Usowicz, J.E. and Johari, H., An Experimental Study of Isolated Turbulent Flame Puffs with a Co-Flow, AIAA Paper 2000-0813, 1-11.